Friction **7**(3): 237–245 (2019)
https://doi.org/10.1007/s40544-018-0208-8
ISSN 2223-7690
CN 10-1237/TH
RESEARCH ARTICLE

Experimental investigation of EHD grease lubrication in finite line contacts

Zhijian WANG[1], **Xuejin SHEN**[1,*], **Xiaoyang CHEN**[1], **Dehua TAO**[1], **Lei SHI**[1], **Shuangbiao LIU**[2]

[1] *School of Mechatronics Engineering and Automation, Shanghai University, Shanghai 200072, China*

[2] *Caterpillar Inc, 100 Sl White Blvd, LaGrange , GA 30241, USA*

Received: 24 April 2017 / Revised: 15 August 2017 / Accepted: 29 January 2018

Abstract: The objective of this study was to investigate the grease-lubricated film-forming mechanisms in the finite line contact and to improve the grease-lubricated finite line contact's film-forming capacity. An elastohydrodynamic lubrication (EHL) test rig with two interferometry microscopes, which could simultaneously monitor two different contact locations in the finite line contact, was constructed in order to study the influences of the grease thickener formulation on the film thickness and lubrication condition. By using the relative light intensity method, the thickness maps of the grease-lubricated film were calculated from the interferometer images captured by the two microscopes. The test results revealed that the grease thickener's formulation had remarkable effects on film formation and the perturbation of film thickness. For the lithium-based grease, the film's thickness near the two ends of the roller was prone to severe perturbation caused by the conglomeration of clumps that were hard to shear. For the aluminum-complex-based grease, the fibers tended to accumulate in the middle of the roller rather than at the two ends. The urea-based grease could be easily sheared into smaller particles. In addition to the straight-line profile rollers, the logarithmic profile rollers were tested and found to effectively enhance the axial grease flow, increase the axial shear stress, and thus shear more fibers into particles within the contact area.

Keywords: EHL; finite line contact; grease; film thickness

1 Introduction

Various greases have been used extensively to lubricate moving components such as gears and rolling element bearings. Several general studies have shown that approximately 90% of rolling element bearings are grease-lubricated [1]. Therefore, it is important to understand the grease lubrication mechanism and to optimize the formulation of grease such that its components may operate smoothly for a sufficient amount of time. Because the majority of these moving components are designed to operate in elastohydrodynamic (EHD) contact (either point contact or line contact), it is useful to study the film-forming mechanisms of greases in an EHD contact with complicate rheological behavior. The film-forming capacity of greases is different from that of lubrication oils, and depends mainly on the formulation of grease, including the thickener's concentration and type, base oil viscosity, rheological and channeling characteristics, base oil type, and application conditions [2]. Cousseau et al. [3] measured the film thickness with greases, bleed oils, and base oils, respectively. They proposed using of the bleed oil properties to predict the grease film thickness under full film conditions. Cann et al. [4] created a simple intuitive diagram to explain the grease film formation mechanism. First, the bulk grease started to decompose into clumps, including the entangled fibers and associated base oil, at a certain distance from the contact area. Then, these

* Corresponding author: Xuejin SHEN, E-mail: Shenxj@t.shu.edu.cn

clumps sheared further and decomposed into smaller units as they entered the contact area, where they eventually generated individual fibers.

Many theoretical and experimental studies have been conducted in order to capture the film-forming behaviors of different greases. In terms of theoretical work, grease rheological properties at low shear rates are generally predicted by Bingham [5] or Herschel-Bulkley [6] models. The Herschel-Bulkley model is essentially a three-parameter rheological equation including the yield shear stress, plastic viscosity, and a rheological grease parameter. Numerical analyses utilizing the Herschel-Bulkley model, such as that of Kauzlarich and Greenwood [7], and Karthikeyan et al. [8], have shown that there is a plug layer in the conjunction where the shear stress is small. Yang and Qian [9] developed a grease-lubricated film-forming model by applying the Bingham rheological equation for elliptical contacts. Their results indicated that the plastic viscosity of the grease influenced the thickness of the film significantly, while the influence of the yield stress was negligible. Thus far, however, a single rheological equation has not been able to properly describe the rheological behavior and flow mechanism of all lubricating greases, owing to differences in the manufacturing process, additives, and type/concentration of the thickener. To a certain extent, the lack of a satisfactory rheological model for grease restricts the application of grease EHD theoretical models to a broader field of engineering applications. Moreover, starvation often occurs with grease lubricated components if the time for the bleeding oil to reflow from the original bulk grease is not sufficient. Therefore, an experimental investigation of the grease lubricated EHD contact has often been used to explain and predict the lubricating behaviors of grease under actual operating conditions. Hurley and Cann [10] first investigated the effect of rolling speed on the film-forming capacity and found that the grease-lubricated film thickness increased with the decrease in the rolling speed at low speed. The thicker film observed at low speed was attributed to the agglomeration of thickener material. A similar phenomenon has also been observed by other researchers. Morales-Espejel et al. [11] developed an empirical model to predict the film thickness of grease at low speed based on extensive experimental work by Cen et al. [12]. Cyriac et al. [13] investigated the influence of rheology and grease formulation (thickener microstructure and concentration) on the grease-lubricated film formation under fully flooded conditions at medium speeds. They reported that larger thickener particles caused the formation of thinner film. However, this was not the case for smaller thickener particles with the same thickener concentration. The opposite trend was observed by Cousseau et al. [14], who investigated the variation of film thickness under starved lubrication over longer test periods. Thus, the effect of the thickener type on the thickness of the grease film may depend on the lubrication conditions.

It should be noted that most of the above mentioned studies are based on point or elliptical contacts. Additionally, only a few studies have investigated the grease-lubricated finite line. To the authors' knowledge, an experimental investigation on the variation of film-forming capacity at different line contact locations simultaneously, has not been reported in the literature. The film-forming capacities of grease are different with different roller sections because of differences in the local grease flow. Thus, more information can be obtained from such an investigation. In this study, an experimental device with two interferometry microscopes was developed in order to observe two different contact areas simultaneously. The film thickness maps were calculated from the interferometer images by the relative light intensity method. These maps in the different contact areas were analyzed in order to gain insights into the film-forming mechanism. The influence of the thickener type and content under various operating conditions was investigated with different speeds, loads, and roller profiles. The results revealed that the grease thickener's formulation exerted a remarkable influence on the film formation and perturbation of the film's thickness. It was observed that the perturbation was more severe at the end regions, rather than at the middle region of the rollers.

2 Test rig and test conditions

2.1 Testing rig

A testing rig with two interferometry microscopes was constructed in order to investigate the grease

lubrication in the finite line contacts. These two microscopes can simultaneously monitor the dual lubrication areas of the testing rollers. Thus, the influence of the grease thickener formulations on the film thickness and lubrication condition could be investigated under different working conditions. The schematics and a picture of the apparatus are shown in Figs. 1–3. A cylindrical 52100 steel roller was loaded against a glass plate, which was driven by a motor and crank train mechanism horizontally above the test roller. The glass plate maintained constant speed for 4–8 s when moving from one side to the other. The dimensions of the test roller were 5 mm in diameter and 15.8 mm in length, with a surface roughness of Ra < 50 nm after grinding. The glass plate was 200 mm in length, 12 mm in thickness, 30 mm in width, and had a surface roughness of Ra < 5 nm. The elastic modulus of the glass plate was 88 GPa. Two microscopes were installed above the glass plate in order to observe the different contact areas illuminated by the two red light sources. In order to achieve better light interference, a thin chromium film with a thickness of 3 nm was coated onto the bottom surface of the glass plate to enhance the reflection of the light. Two high-speed video cameras were installed on two microscope eyepieces and were linked to a computer, where the film thickness interference images were recorded. To calculate the film thickness from the interference images, the order of the interference image in the contact area had to be carefully evaluated by reviewing their frames. Then, the relative light intensity principle could be applied in order to calculate and generate the film thickness maps. Luo et al. [15] provided a detailed explanation of this method. Equation (1) was applied in order to determine the film thickness, as follows:

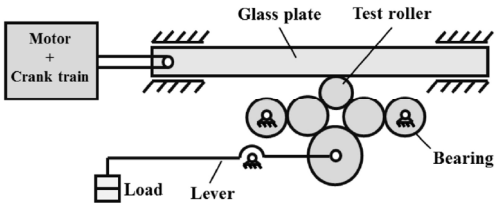

Fig. 1 Diagram of mechanical system.

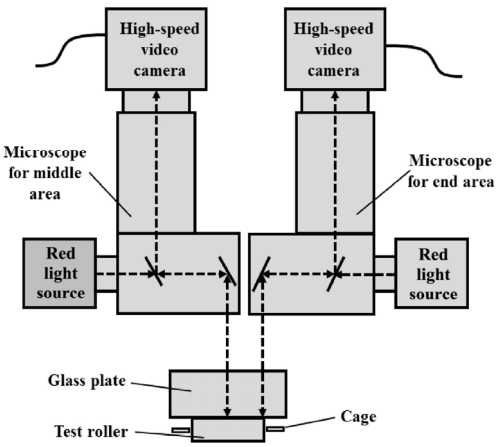

Fig. 2 Diagram of film thickness measuring system.

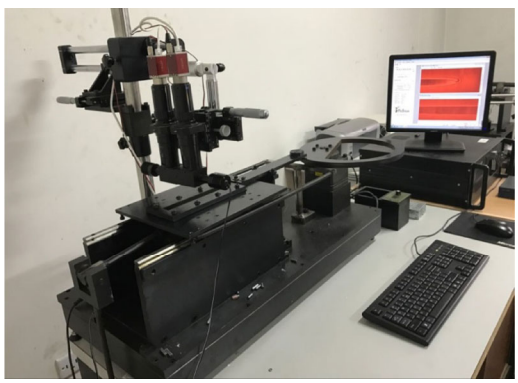

Fig. 3 Finite-line contact EHD device.

$$h=\frac{\lambda}{4\pi k}\left[\left(n+\left|\sin\frac{n\pi}{2}\right|\right)\times\pi+\arccos(\bar{I})\times\cos(n\pi)-\arccos(\bar{I}_0)\right] \quad (1)$$

where λ is the wave length of the incident light (600 nm for the red light), k is the reflective index of the lubricant (k = 1.47), n is the interference order, $\bar{I}$ is the relative interference light intensity, $\bar{I}_0$ is the relative light intensity when the film thickness is zero, and h is the film thickness.

During the setup of the test rig, two microscopes were used to observe the lubrication at both ends. The measured interference images were used to guide the adjustment, which ensured that the roller and glass plate were properly aligned and that the motions of the components in this test rig were smooth.

2.2 Test conditions and lubricants

All measurements were recorded under an ambient temperature of 16 °C. The load between the steel

roller and the glass plate varied from 248 N to 653 N, which resulted in a maximum Hertizan pressure (p_{max}) ranging from 0.358 GP to 0.580 GPa. The motion of the steel roller was pure rolling. During the period of constant speed, the rolling speed (u) was adjusted from 0.015 m/s to 0.046 m/s. Eight types of greases were used in the following experiments in order to demonstrate the effect of the different thickener types and thickener concentration on the film-forming behavior. All of the greases were made from the same mineral oil (343 mm^2/s at 40 °C) and their compositions are listed in Table 1. Prior to each test, all of the specimens and related parts were cleaned by an hydrous ethanol and dried. The grease was smeared uniformly on the glass plate to a thickness of 0.2 mm to 0.4 mm, and no additional grease was supplied during the test. To reduce the effect of starvation, the experimental results were observed during the first two revolutions.

Two roller profiles were used in this study: (a) a straight line profile with an end chamfer and (b) a logarithmic profile, as shown in Fig. 4, where δ is a crown drop referring to the reduction of the radius. Rollers with two different crown drops were manufactured and tested with different greases. However, only the results obtained with #C grease are reported in this paper.

Table 1 Formulation of tested greases.

Grease	Thickener type	Thickener concentration (wt%)	Oil type (viscosity at 40 °C)
A	Aluminum complex	6%	Mineral oil (343 mm^2/s)
B	Aluminum complex	8%	
C	Aluminum complex	10%	
D	Lithium	6%	
E	Lithium	8%	
F	Lithium	10%	
G	Urea	10%	
H	Urea	13%	

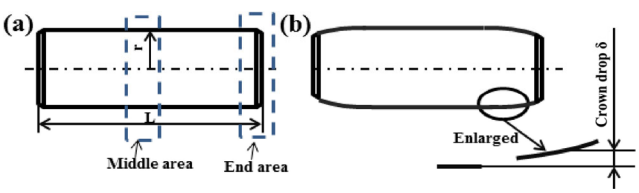

Fig. 4 Cylindrical roller profiles.

3 Results and discussion

3.1 Film thickness of roller's middle and end regions

Figure 5 shows a set of example film thickness interference images at the middle and end areas of the roller lubricated with #C, #F, and #G greases with the same thickener concentration (10%), but with different thickener types. The roller used here had a straight line profile. The two observation locations are illustrated in Fig. 4(a). By comparing the interference images between the middle and end of the roller for these three types of grease, it was found that the light intensity was lower in the middle of the contact area. This implied that more soap fibers accumulated in the middle of the roller. This occurred because the axial pressure gradient ($\partial p / \partial x$) was approximately zero in the middle of the roller, which restricted the grease from flowing to the side. Additionally, when there was no grease lubrication, the contact pressure in the middle of the roller was lower than that at the end of the roller. This reduced the shear stress as shown in Fig. 6. With less shear stress, more fibers could accumulate in the middle of the roller, which resulted in a slightly darker fringe in the central areas. For the aluminum-complex-based grease (#C), the

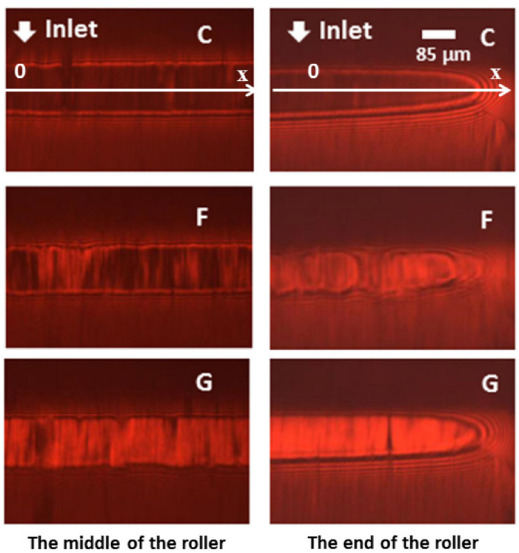

Fig. 5 Interference images of three different types of grease (u = 15 mm/s, p_{max}=0.58 GPa, straight line profile).

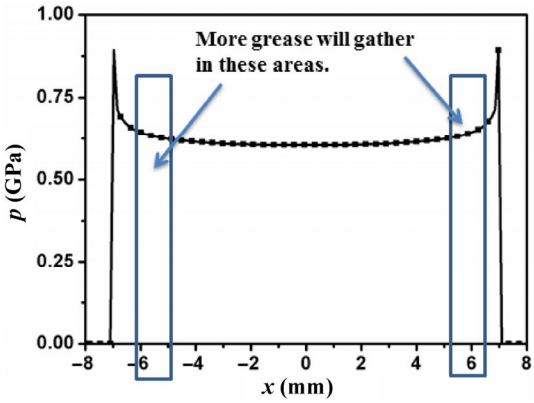

Fig. 6 Schematic of dry contact pressure for straight line profile roller.

contacts were not severely perturbed, neither in the middle nor at the end of the roller. This indicated the existence of very few large soap clumps within the contact area. For the lithium-based grease (#F), the film thickness interference images were severely distorted at the end indicated that the contact area may have had a significant amount of large soap clumps. Additionally, the film thickness interference images were only slightly perturbed in the middle of the roller. This raised the following question: why is it that larger soap clumps can survive at the end but not in the middle of the roller? The reason is probably related to the large amount of grease that accumulates close to the ends of the roller during its operation, as shown in Fig. 6. If the clumps are difficult to shear into fibers, the film thickness interference images should appear distorted. For the urea-based grease (#G), most of the grease in the contact area could be fully sheared since its center area had the brightest fringes. Figure 7 shows the film thickness along the axial direction of the roller with three types of grease. The film thickness of the lithium-based greases (#F) at the end of the roller was not plotted because the film-thickness interference image was severely perturbed. By comparing these three types of grease, it was found that the aluminum-complex-based grease formed the thickest film, followed by the lithium-based grease, and then the urea-based grease, when the speed was equal to 15 mm/s. It should be noted that these conclusions are valid only for the testing greases considered in this study, since different manufacturing processes can strongly affect the mechanical behavior of lubricating grease [16].

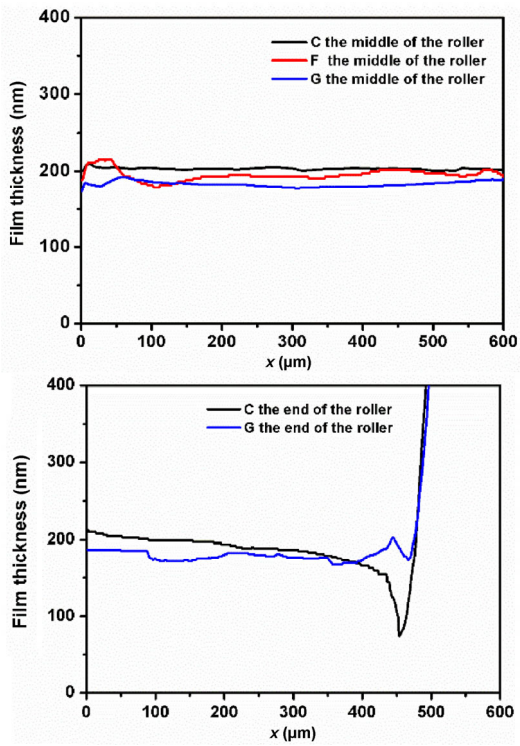

Fig. 7 Film thickness along axial direction with different thickener types (u = 15 mm/s, p_{max}=0.58 GPa, straight line profile).

3.2 Effects of roller profile

Figure 8 shows the interference images of film thickness at the middle and end areas of the roller lubricated with the aluminum-complex-based grease

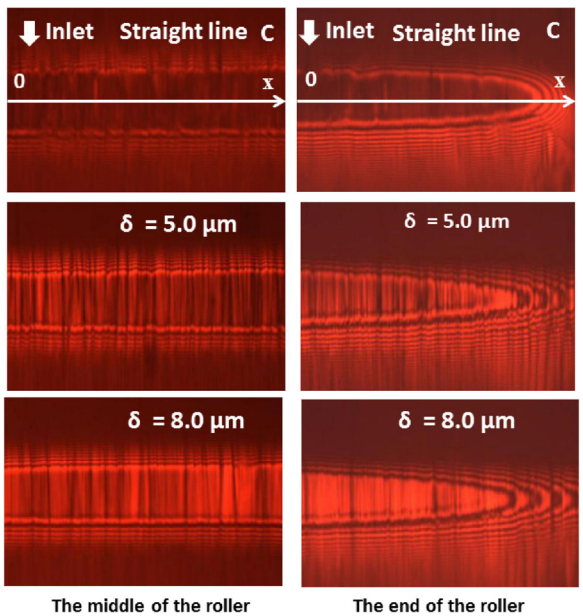

Fig. 8 Interference images captured using different profile rollers (u = 15 mm/s, p_{max}=0.58 GPa).

by using the two profiled rollers. In comparison to the logarithmic profile roller, the light intensity of the interference images with the straight line roller was lower, which indicates that it may have had a layer of fibers within the contact area of the straight line roller. For the logarithmic profiled roller, as the crown drop increased, the brightness inside the contact region increased and the fluctuation of the brightness became less frequent. This indicates that a larger logarithmic profile can effectively enhance the grease flow, increase the axial shear stress, and reduce the number of soap fibers in the contact area. The contact pressure schematic for the logarithmic profile roller without grease lubrication is shown in Fig. 9. Moreover, the obtained pressure gradient supported the above-mentioned interpretation. Figure 10 shows the film thickness along the axial direction in the contact area. It was found that the logarithmic profiled roller with a larger crown drops lightly reduced the film thickness and the constriction location moving towards the middle of the roller.

3.3 Effects of thickener concentration

Figure 11 shows the film-thickness interference images for different thickener concentrations. As the concentration of the aluminum-complex-based grease used for lubrication increased, more soap fibers appeared in the contact area, which may have increased the frictional torque [17]. In the case of the lithium-based grease, the large soap clumps tended to agglomerate at the end of the roller with a higher thickener concentration (#F). These soap clumps caused the severe perturbation of the film thickness and

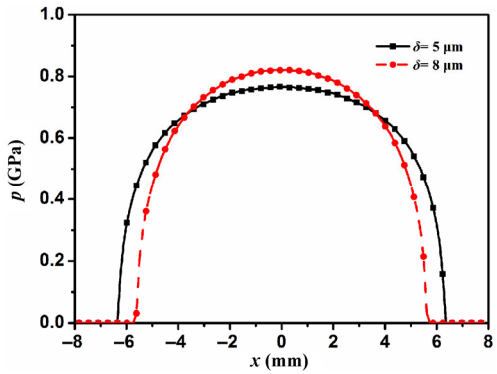

Fig. 9 Schematic of dry contact pressure for logarithmic profile roller.

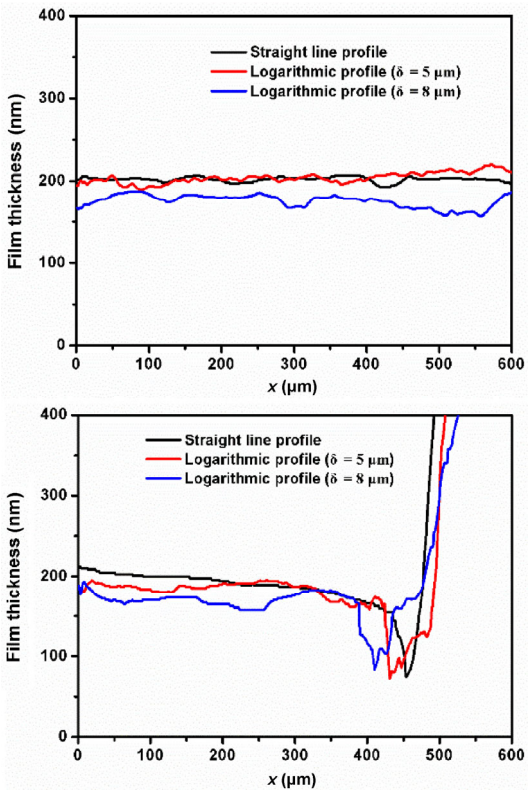

Fig. 10 Film thickness along axial direction with different profile rollers (u = 15 mm/s, p_{max}=0.58 GPa).

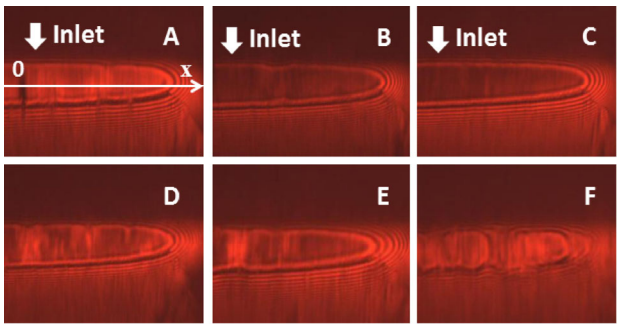

Fig. 11 Interference images for aluminum-complex-based grease and lithium-based grease with different thickener concentrations (u = 15 mm/s, p_{max}=0.58 GPa, straight line profile).

produced a local pressure spike, which may have influenced the noise level and could have increased the risk of pitting damage [18]. Figure 12 shows the film thickness of the aluminum-complex-based grease and the lithium-based grease with various thickener concentrations. It was found that the film thickness increased slightly with a higher thickener concentration. Thus, a proper thickener to base oil ratio has to be identified in order to balance the grease film-forming capacity, frictional torque, and sound requirements.

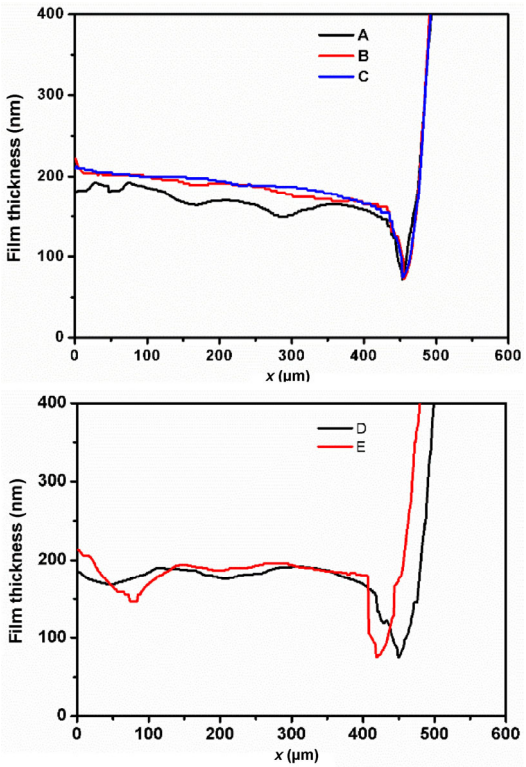

Fig. 12 Film thickness for aluminum-complex-based grease and lithium-based grease with different thickener concentrations (u = 15 mm/s, p_{max}=0.58 GPa, straight line profile).

3.4 Effects of speed

Figure 13 shows the film-thickness interference images of three different types of grease at different speeds: 15 mm/s and 30 mm/s. For the aluminum-complex-based grease, the light intensity in the contact area became brighter as the speed increased (as shown in Fig. 13), while the reduction of the soap fibers caused the reduction of the film thickness (as shown in Fig. 14). For the lithium-based grease, although the order of the interference fringe did not change as the

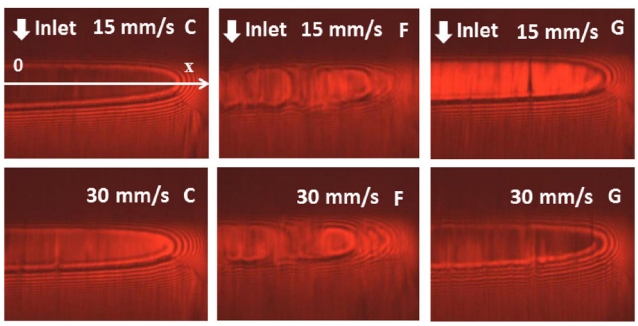

Fig. 13 Interference images of three types of grease at different speeds (p_{max}=0.58 GPa, straight line profile).

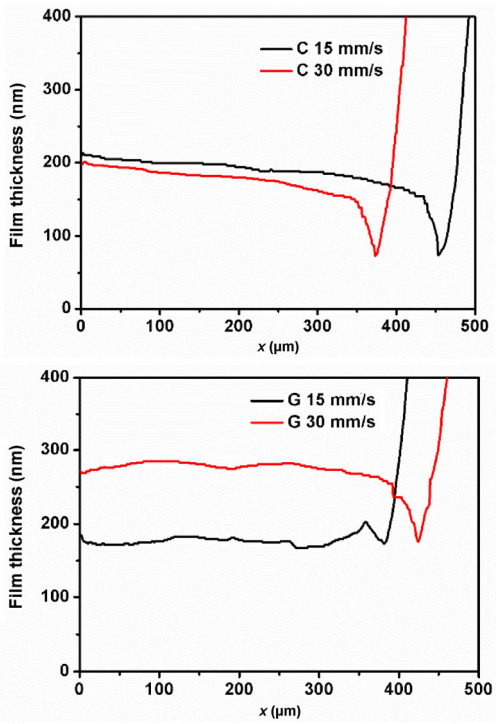

Fig. 14 Film thickness for aluminum complex-based and urea-based grease at different rolling speeds (p_{max}=0.58 GPa, straight line profile).

speed increased, the perturbation of the film thickness slightly weakened, which indicated that either the amount of soap clumps entering into the contact area reduced or the influence of the soap clumps on the perturbation of the film thickness weakened as a result of the film thickness increasing. For the urea-based grease, the order of the interference fringe in the contact area increased with speed, which indicates a thicker film, as shown in Fig. 14.

3.5 Effects of load

Figure 15 shows the film-thickness interference images for of three types of grease (10% thickener concentration) under different load levels. The corresponding maximum Hertzian pressures were 0.358 GPa, 0.440 GPa, and 0.520 GPa. For all greases, the contact area increased in the rolling direction as the load increased. For the aluminum-complex based grease and the lithium-based grease, the film interference images fluctuated severely under a light load (0.358 GPa). This was attributed to the presence of large clumps. However as the load increased, the fluctuation reduced. Figure 16 shows the film thickness

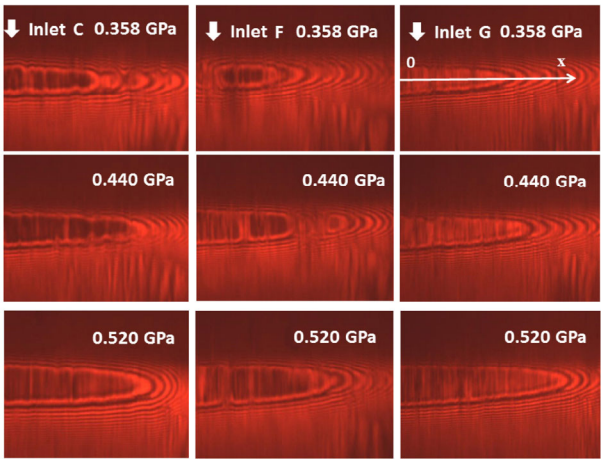

Fig. 15 Interference images of three types of grease under different loads (u = 15 mm/s, straight line profile).

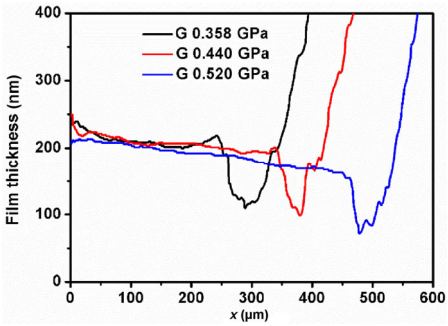

Fig. 16 Film thickness for urea-based grease under different loads (u = 15 mm/s, straight line profile).

of the urea-based grease under different loads. Similar to the film thickness distribution in an oil-lubricated EHD contact, it was found that the film thickness of the grease-lubricated EHD contact remained essentially unchanged, with the exception of the constriction position. Moreover, the film-forming capacity of the grease was not remarkably influenced by the load.

4 Conclusions

In this study, a finite-line contact EHL test rig with two interferometry microscopes was constructed. This rig was able to measure the film thickness at two locations simultaneously. Three different thickener types, namely lithium, aluminum complex, and urea, with different concentrations, were used to analyze the grease lubrication film-forming mechanism in the finite line contacts. The grease lubrications were experimentally investigated under different load levels, rolling speeds, and roller profiles. The conclusions drawn from this study are as follows:

(1) Unlike the point contact, the film-forming capacity of the finite line contact was distinct between the middle and the end of the roller. More soap fibers accumulated at the middle region and contributed to the thicker film thickness, whereas large soap clumps accumulated near the end of the roller and caused severe perturbation to the film thickness.

(2) The type of thickener influenced the lubrication under the test conditions used in this study. For the lithium-based grease, the end of the roller was prone to the production of severe perturbation. For the aluminum-complex-based grease, the thickest film formed because of the existence of the thickener fibers.

(3) At a speed as low as 15mm/s, the film thickness increased with the concentration of the thickener. However, a higher thickener concentration caused severe perturbation to the film thickness, which led to a high noise level.

(4) The logarithmic profile roller enhanced the axial flow of the grease, increased the shear stress in the axial direction, and reduced the number of fibers in the contact area.

(5) In this study, the light load and low speed were prone to the severe fluctuation of the film near the end of the roller, which resulted in a high noise level.

Acknowledgements

This work was funded by the twelfth five-year projects of China for science and technology under Contract D50-0109-12-001 and the Key Innovational Program of Shanghai Municipal Education Commission (No. 11ZZ89). The financial supports are greatly appreciated. The authors would like to thank Dr. Qingtao Yu of Aviation Industry Corporation of China for valuable suggestions.

References

[1] Lugt P M. *Grease Lubrication in Rolling Bearings*. New York (USA): John Wiley & Sons, 2013.

[2] Vengudusamy B, Kuhn M, Rankl M, Spallek R. Film forming behavior of greases under starved and fully flooded EHL conditions. *Tribol Trans* **59**(1): 62–71 (2016)

[3] Cousseau T, Björling M, Graça B, Campos A, Seabra J, Larsson R. Film thickness in a ball-on-disc contact lubricated with greases, bleed oils and base oils. *Tribol Int* **53**: 53–60 (2012)

[4] Cann P M, Williamson B P, Coy R C, Spikes H A. The behaviour of greases in elastohydrodynamic contacts. *J Phys D* **25**(1A): A124–A132 (1992)

[5] Bingham E C. *Fluidity and Plasticity*. New York (USA): McGraw-Hill Book Co, 1922.

[6] Herschel W H, Bulkley R. Measurement of consistency as applied to rubber-benzene solutions. *Am Soc Test Proc* **26**: 621–633 (1926)

[7] Greenwood J A, Kauzlarich J J. Inlet shear heating in Elastohydrodynamic lubrication. *J Lubr Technol* **95**(4): 417–423 (1973)

[8] Karthikeyan B K, Teodorescu M, Rahnejat H, Rothberg S J. Thermoelastohydrodynamics of grease-lubricated concentrated point contacts. *Proc Inst Mech Eng Part C J Mech Eng Sci* **224**(3): 683–695 (2010)

[9] Bordene L, Dalmaz G, Chaomleffel J P, Vergne F. A study of grease film thicknesses in elastorheodynamic rolling point contacts. *Lubr Sci* 2(4): 273–284 (1990)

[10] Hurley S, Cann P M. Grease composition and film thickness in rolling contacts. *NLGI Spok* **63**(4): 12–22 (1999)

[11] Morales-Espejel G E, Lugt P M, Pasaribu H R, Cen H. Film thickness in grease lubricated slow rotating rolling bearings. *Tribol Int* **74**: 7–19 (2014)

[12] Cen H, Lugt P M, Morales-Espejel G. On the film thickness of grease-lubricated contacts at low speeds. *Tribol Trans* **57**(4): 668–678 (2014)

[13] Cyriac F, Lugt P M, Bosman R, Padberg C J, Venner C H. Effect of thickener particle geometry and concentration on the grease EHL film thickness at medium speeds. *Tribol Lett* **61**: 18 (2016)

[14] Cousseau T, Graça B, Campos A, Seabra J. Grease aging effects on film formation under fully-flooded and starved lubrication. *Lubricants* **3**(2): 197–221 (2015).

[15] Luo J B, Wen S Z, Huang P. Thin film lubrication. Part 1: Study on the transition between EHL and thin film lubrication using a relative optical interference intensity technique. *Wear* **194**(1–2): 107–115 (1996)

[16] Franco J M, Delgado M A, Valencia C, Sánchez M C, Gallegos C. Mixing rheometry for studying the manufacture of lubricating greases. *Chem Eng Sci* **60**(8–9): 2409–2418 (2005)

[17] Oikawa E, Inami N, Hokao M, Yokouchi A, Sugimura J. Bearing torque characteristics of lithium soap greases with some synthetic base oils. *Proc Inst Mech Eng Part J J Eng Tribol* **226**(6): 575–583 (2012)

[18] Lugt P M. Modern advancements in lubricating grease technology. *Tribol Int* **97**: 467–477 (2016)

Zhijian WANG. He received his bachelor degree in mechanical engineering in 2010 from Jinan University, Shandong, China. At present, he is a PhD candidate in Shanghai University, China. His research interests include the rolling bearing tribology design.

Xuejin SHEN. She received the B.S. degree from Southeast University, China, and Ph.D. degree from Shanghai University, China, all in mechatronic engineering, in 1984, 2007, respectively. She became an associate professor in 2001, a full professor in 2009, in the Department of Mechanical Automation Engineering, Shanghai University. She is a senior member of Chinese Mechanical Engineering Society. Her research interest includes the performance analysis of rolling bearings, EHL of finite line contact, and mechanical model of MEMS.